

NUMERICAL INVESTIGATION OF THE TRANSIENT SPRAY COOLING PROCESS FOR QUENCHING APPLICATIONS

by

**Jakov BALETA^{a*}, Fengsheng QI^b, Marija ZIVIC^c,
and Martina LOVRENIC-JUGOVIC^a**

^a Faculty of Metallurgy, University of Zagreb, Sisak, Croatia

^b School of Metallurgy, Northeastern University, Shenyang, China

^c Mechanical Engineering Faculty in Slavonski Brod, University of Osijek, Osijek, Croatia

Original scientific paper

<https://doi.org/10.2298/TSCI180120261B>

Water spray quenching distinguished itself as a promising method for industry production, especially for the parts which require good mechanical strength while simultaneously retaining the initial toughness. Studies have shown that the heat transfer process during the spray quenching is mostly influenced by the spray impingement density, particle velocities and sizes. The application of advanced numerical methods still plays insufficient role in the development of the production process, in spite of the fact that industry today is facing major challenges that can be met only by development of new and more efficient systems using advanced tools for product development, one of which is CFD. Taking the above stated, the object of this research is numerical simulation of spray quenching process in order to determine validity of mathematical models implemented within the commercial CFD code Fire, especially droplet evaporation/condensation and droplet-wall heat transfer model. After review of the relevant literature suitable benchmark case was selected and simulated by employing discrete droplet method for the spray treatment and Eulerian approach for the gas phase description. Simulation results indicated that existing droplet/wall heat transfer model is not able to reproduce heat transfer of dense water spray. Thus, Lagrangian spray model was improved by implementing experimental correlation for heat transfer coefficient during spray quenching. Finally, verification of the implemented model was assessed based on the conducted simulations and recommendations for further improvements were given.

Key words: *spray quenching, CFD, spray/wall interaction, heat transfer*

Introduction

The need for high density heat flux dissipation exists in many areas such as metallurgy, electronic devices [1, 2], aerospace engineering, nuclear industry, X-ray medical devices, high power lasers, etc. Spray cooling is the most effective direct cooling technique [3]. It provides homogenous temperature distribution across the cooling surface. Applications of spray cooling can be divided into two major groups: low temperature steady-state cooling and high temperature transient cooling [4]. In literature there is abundance of experimental studies, but it is very scarce in numerical description of spray quenching. For example, Yao and Cox [5] developed correlations for spray heat transfer effectiveness and Leidenfrost tempera-

* Corresponding author; e-mail: baleta@simet.hr

ture based on the Reynolds and Weber numbers, where spray mass velocity was substituted in their definition instead of droplet velocity. Puschmann and Specht [6] investigated influence of water impingement density, distribution of drop diameter, distribution of drop velocity, surface temperature and air flow in spray cooling with twin fluid nozzle. Jha *et al.* [7] experimentally studied air atomized spray cooling of a moving steel plate by varying plate velocity and water flow rate. Chen *et al.* [8] experimentally investigated influence of mean droplet flux, sauter mean diameter and droplet velocity on spray cooling effectiveness at critical heat flux. The same authors in one of their earlier works [9] investigated the effects of same parameters on critical heat flux. Silk *et al.* [10] performed spray cooling heat flux measurements on three different enhanced surfaces with different spray axis inclination. Ciofalo *et al.* [11] performed experimental investigation of spray cooling in nucleate boiling and single-phase heat transfer regimes. Visaria and Mudawar [12] examined effects of subcooling on critical heat flux of spray cooling and also used experimental data to develop correlation for critical heat flux. Mascarenhas and Mudawar [13] presented overview of correlations found in literature for different heat transfer regimes found in spray quenching process. Al-Ahmadi and Yao [14] conducted extensive experimental investigation for the spray cooling of high-temperature steel using different types of industrial nozzles and varied spray angle, water mass flux and orientation of spray with respect to gravity. Liang and Mudawar [15] performed review of single phase and nucleate boiling regimes in spray cooling and key spray parameters influencing heat transfer performance were identified. Zhao *et al.* [16] developed heat transfer model based on energy conservation that takes into account contribution of five mechanisms during spray cooling: droplet-film impact, film-surface convective heat transfer, heat transfer induced by wall nucleation bubbles and secondary nucleation bubbles, and environmental heat transfer. Shedd and Pautsch [17] made detailed parametric study of heat transfer on prototype of spray impingement cooling system with single and multiple nozzle array. Mascarenhas and Mudawar [18] conducted parametric investigation of spray quenching thick metal alloy tubes based on derived analytical model for the determination of the shape and size of the spray impact zone. Mudawar and Estes [19] investigated spray cooling of a hot surface by varying nozzle-to-surface distance and developed theoretical model that was able to predict spray volumetric flux distribution across the impinging surface. Visaria and Mudawar [20] developed model that predicts spatial distribution of volumetric flux and spray impact area as a function of spray inclination. In the same paper they also investigated effect of spray inclination, flow rates and subcooling on spray cooling and critical heat flux.

Tseng *et al.* [21] gave an overview of heat transfer coefficient correlations for spray cooling. Most of the correlations from the literature are presented in empirical form which can hinder underlying physics. Based on the conducted literature review it can be stated that spray cooling is highly complex process dependent on large number of parameters [15]: liquid type, liquid saturation temperature, liquid subcooling, thermophysical properties of liquid, ambient pressure, thermophysical properties of surrounding vapor/gas, surface parameters, flow parameters, and geometrical parameters of spray nozzle. However, following three parameters play crucial role in in spray cooling: droplet size, droplet velocity, and volumetric flux.

The CFD is today being employed for numerical modelling of various physical processes with pronounced practical significance, for example: heat transfer of a turbulent jet impinging on a moving plate [22], numerical investigation of film cooling [23], use of auto-ignition tabulation for complex chemistry combustion mechanisms [24], design of top combustion hot blast stove [25], influence of biofuel addition to diesel fuel [26] and numerical analysis of cement calciner [27]. Regarding spray cooling, one of rare numeric studies was

presented in [28] where authors implemented correlation of Wendelstorf *et al.* [29] for heat transfer coefficient as a part of enhanced Euler-Eulerian model for the simulation of spray quenching process. It provided solid basis for numerical implementation because it encompasses wide range of experimental conditions and is only depended upon two parameters, namely impingement density and temperature difference between wall and spray droplets.

Based on the presented overview, the object of this research is twofold. First, numerical simulation of spray quenching process is conducted in order to determine validity of mathematical models implemented within the commercial CFD code Fire, especially droplet-wall heat transfer model. It was found that current droplet/wall heat transfer model is unable to cope with effects of pronounced wall wetting even in the case of fairly dilute spray produced by air assisted atomizer. Thus, Lagrangian spray model was improved by implementing experimental correlation for heat transfer coefficient during spray quenching. First results indicate favorable outcome.

Mathematical model

This section presents some basics of most important underlying mathematical models including solution of the gas phase using general transport equation, Lagrangian description of spray inside computational domain, model for spray interaction with wall including heat transfer and finally different heat transfer regimes with correlation from Wendelstorf *et al.* [29].

Gas phase

Mass conservation law for differential element of fluid in Cartesian co-ordinate system can be expressed by following equation:

$$\frac{\partial \rho}{\partial t} + \frac{\partial}{\partial x_j} (\rho u_j) = 0 \quad (1)$$

where ρ is the fluid density, t represents time, x_j are the x-Cartesian co-ordinates and u_j is the velocity vector components. For incompressible fluid, eq. (1), states that the divergence of velocity is equal to zero.

Momentum conservation law for differential, incompressible element of Newtonian fluid can be written in the following form:

$$\frac{\partial}{\partial t} (\rho u_i) + \frac{\partial}{\partial x_j} (\rho u_i u_j) = -\frac{\partial p}{\partial x_i} + \mu \frac{\partial^2 u_i}{\partial x_j \partial x_j} + \rho f_i \quad (2)$$

Equations (1) and (2) are also known as Navier-Stokes equations.

Energy conservation law is written:

$$\frac{\partial}{\partial t} (\rho i) + \frac{\partial}{\partial x_j} (\rho i u_j) = -p \frac{\partial u_j}{\partial x_j} + \frac{\partial}{\partial x_j} \left(\lambda \frac{\partial T}{\partial x_j} \right) + \rho f_i v_i + \frac{\partial (\tau_{ji} v_i)}{\partial x_j} \quad (3)$$

where i is specific internal energy of fluid.

The observed commonalities between presented governing equations enable introduction of a general scalar variable φ , with whom general conservative form of all fluid flow equations can be stated:

$$\frac{\partial}{\partial t} (\rho \varphi) + \frac{\partial}{\partial x_j} (\rho \varphi u_j) = \frac{\partial}{\partial x_j} \left(\Gamma_\varphi \frac{\partial \varphi}{\partial x_j} \right) + S_\varphi \quad (4)$$

In the previous equation four characteristic members can be distinguished each with distinct physical meaning: first term on the left hand side represents time rate of change of scalar variable φ , second term on the left hand side is convective transport of the same variable, first term on the right hand side describes diffusional transport of φ , whilst the last term of the equation is source/sink of the variable φ due to various other mechanisms. General transport eq. (4) represents foundation for the numerical theory of CFD. In this work conservation equations of mass, momentum and energy based on Reynolds averaging were solved.

Lagrangian spray

Discrete droplet method (DDM) [30] still remains industrial standard for numerical spray description [31] in spite the fact that Euler Eulerian size of class model has gained attention recently for specific tasks, such as computation of dense sprays [32]. The DDM is grouping droplets of the same size and physical properties into parcels and numerically solves only differential equations of parcels, thus enabling more efficient calculations. Otherwise, it would be computationally impossible to solve differential equations for every spray droplet.

Lagrangian description of motion uses initial conditions for every parcel and describes the motion of particles inside computational domain by relying onto Newton's second law of motion which states that the net force on an object is equal to the rate of change of its linear momentum in an inertial reference frame:

$$m_d \frac{du_{id}}{dt} = F_{idr} + F_{ig} + F_{ip} + F_{ib} \quad (5)$$

where m_d and u_{id} are droplet mass and droplet velocity, F_{idr} is the drag force, F_{ig} represents gravity and buoyancy, F_{ip} is the pressure force and F_{ib} takes into account other external forces. Drag force and gravity effects are only relevant for spray cooling application. Therefore follows:

$$m_d \frac{du_{id}}{dt} = F_{idr} + F_{ig} \quad (6)$$

u_{id} could be obtained by integrating above equation and afterwards it is used to finally calculate parcel trajectory:

$$\frac{dx_{id}}{dt} = u_{id} \quad (7)$$

Spray/wall interaction model

Experimental investigation carried out by Kuhnke [33] revealed four different regimes of spray-wall interactions depending on two non-dimensional parameters, namely non-dimensional wall temperature and non-dimensional droplet velocity. Non-dimensional temperature is ratio between wall temperature T_w and droplet saturation temperature T_s :

$$T^* = \frac{T_w}{T_s} \quad (8)$$

Non-dimensional droplet velocity is defined as:

$$K = \frac{(\rho_d D_d)^{3/4} u_{d,\perp}^{5/4}}{\sigma_d^{1/2} \mu_d^{1/4}} \quad (9)$$

where ρ_d is the droplet density, D_d represents droplet diameter, $u_{d,\perp}$ is the wall normal component of the droplet velocity, σ_d is a surface tension and μ_d is the dynamic viscosity of droplet.

By using non-dimensional wall temperature and non-dimensional droplet velocity it is possible to identify following droplet wall interaction regimes: deposition, splash, rebound, and thermal breakup. More details can be found in [33].

Wruck heat transfer model

Heat transfer between impinged spray droplet and hot wall is treated with model developed by Wruck [34] which conveniently utilizes the four regime map of the Kuhnke model. It is one of the aims of this study to investigate validity of this model for spray quenching applications.

Heat transferred to the droplet is calculated taking into account heat penetration coefficients b of droplet and wall, temperature difference between wall and droplet, and contact time:

$$Q = A_{\text{cont}} \frac{2\sqrt{t_{\text{dc}}}}{\sqrt{\pi}} \frac{b_w b_d}{b_w + b_d} (T_w - T_d) \quad (10)$$

Contact time is calculated depending on the non-dimensional droplet velocity defined with eq. (9):

$$K < 40 \quad t_{\text{dc}} = \frac{\pi}{4} \sqrt{\frac{\rho_d D_d^3}{\sigma_d}} \quad (11)$$

$$K > 40 \quad t_{\text{dc}} = \sqrt{\frac{\pi}{2} \left[\frac{\rho_d D_d^5}{\sigma_d u_d^2} \right]^{-0.25}} \quad (12)$$

Quenching heat transfer coefficient

Heat transfer regimes during quenching can be characterized according to temperature difference between surface and cooling water onto: single phase regime, nucleate boiling regime, transition boiling regime and film boiling regime. Heat transfer correlation developed by Wendelstorf *et al.* [29] takes into account wide range of operating conditions and is suitable for dense sprays, for temperature difference >180 °C. In this correlation heat transfer coefficient is only function of temperature difference between droplet and wall, and spray impingement density:

$$\alpha(V_s, \Delta T) = C \left(190 + \tanh\left(\frac{V_s}{8}\right) \left\{ 140 V_s \left(1 - \frac{\Delta T}{72,000} V_s \right) + 3.26 \Delta T^2 \left[1 - \tanh\left(\frac{\Delta T}{128}\right) \right] \right\} \right) \quad (13)$$

In order to assess accuracy of the correlation, its results were compared with experimental results reported in [29], where disc made of 99.3% pure nickel with diameter of 70 mm and 1 mm thickness was cooled from 1200 °C by spraying water. Figure 1 depicts results of this comparison, and it can be readily seen that agreement with experiment improves with increasing spray impingement density and temperature difference. Consequently, correlation is able to better describe high temperature regimes in conditions of abundant spray cooling. Overall, the agreement with experiment is satisfactory and this correlation was basis for heat transfer modeling of spray cooling process in commercial CFD code Fire.

It was implemented in commercial CFD code Fire where heat transfer coefficient calculated according to the correlation from [29] was used for assessment of heat sink of the wall and heat source of the droplet. At this point it should be noted that results of CFD simulation with newly implemented model should be compared with correlation results itself, not

with experiment because it has been proven in fig. 1 that correlation has some discrepancies with respect to experiment. Only matching between CFD and correlation results verifies implemented procedure.

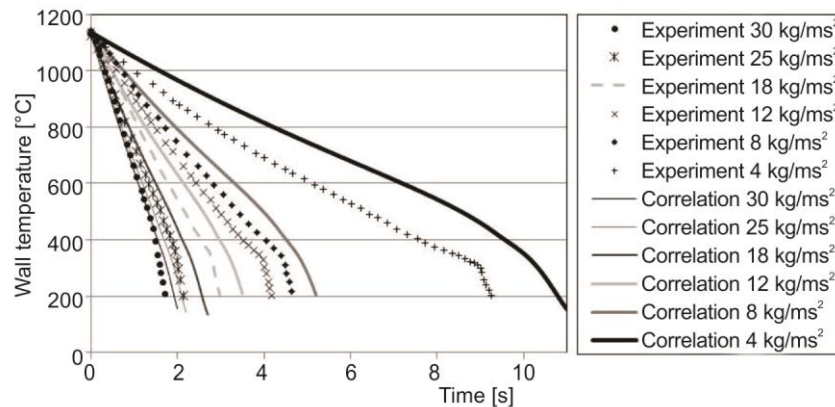


Figure 1. Comparison of correlation for spray cooling with experimental measurements reported in [29]

Numerical simulation settings and results

This section is divided as follows – first, validity of existent heat transfer model described in the previous section was determined on the experimental work carried by Puschmann and Specht [4] and afterwards, newly implemented correlation for heat transfer coefficient was validated against literature quenching curve.

Wruck heat transfer model for quenching applications

In this section the spray calibration results are explained and then calibrated spray was used for the simulation of spray quenching.

Spray calibration

In order to carry out spray calibration, hexahedron mesh was generated with the resolution corresponding to the patternator used in [6], *i. e.* 4.5 mm. For the simulation, default numerical settings in Fire and time step of $10e-4$ s were used. Final calibration results are shown in fig. 2, where it can be noticed fairly good agreement with experimental results.

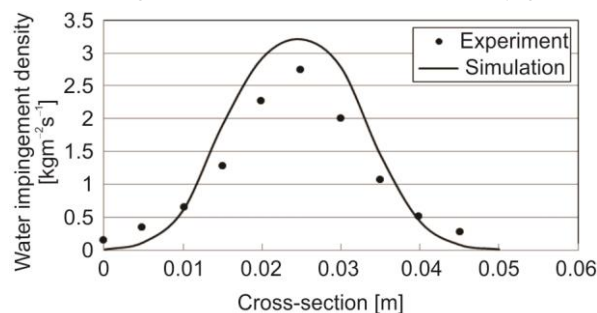


Figure 2. Spray mass distribution – comparison with experimental results

Final set of spray parameters is presented in tab. 1. After spray calibration was completed it was possible to simulate spray quenching process and related heat transfer, results of which are reported in the following section.

Quenching simulation

Main simulation was carried out using experimental conditions reported in [6]. In this work thin metal sheet made of nickel alloy 600 was cooled

Table 1. Results of spray calibration

Spray parameter	Final value after calibration
Spray cone angle	30°
Number of different particle sizes introduced per time step	3
Number of radial parcel release locations on each nozzle hole	2
Number of particles introduced per nozzle ring	6

computational domain constant pressure of 100,000 Pa was imposed. Turbulence was described by well-established k-epsilon model. The domain was initialized with constant temperature of 293.15 K and pressure of 100000 Pa. Implicit time integration was employed to ensure unconditional solution stability. Solution was assumed to converge after residuals of transport equations decrease four orders of magnitude. The pressure velocity coupling was achieved using the combination of semi implicit methods pressure linked equations/pressure implicit split operator (SIMPLE/PISO) algorithms. For the momentum equation minmode relaxed differencing scheme was used with so called blending factor of 0.5 between minmode relaxed and upwind differencing scheme, while central differencing scheme was applied to continuity equation. Finally, upwind differencing scheme was employed for the rest of transport equations. Evaporation of water droplets was described using Abramzon/Sirignano evaporation model [35]. Table 2 represents most important parameters of the *default case*. Droplet size distribution was assumed to be Gaussian with mean value of 8 μm and standard deviation of 3 μm.

Table 2. Default case parameters

	Default case
Spray mass-flow	6 kg/h
Droplet velocity	28 m/s
Heat penetration coefficient	9000 Ws/0.5m ² K
Droplet size	Gaussian PSD, 8 μm
Number of spray wall interaction regimes	4

size and velocity, as well as heat penetration coefficient matching those reported in [6].

Figure 3 shows that different impingement regimes have almost negligible influence to simulation results. Also, droplet size plays only minor role in quenching simulation and only in later stages. Smaller droplets are able to take more heat form the wall and consequently temperature is fairly lower compared to the default case. Experimental results are greatly overestimated in simulation and it seems it remains so in all combinations of different parameters.

Figure 4 confirms findings of previous figure. Higher droplet velocities yield lower heat transfer due to the fact that contact time decreases with increasing velocity. As expected, increase in heat penetration coefficient promotes better cooling. However, neither of simulation cases was able to reproduce experimental heat transfer dynamics. This brings to conclusion that implemented droplet/wall heat transfer model is maybe able to reproduce heat transfer of single droplet, but is unable to cope with effects of pronounced wall wetting, even in the case of fairly dilute spray produced by air assisted atomizer. Also, current model is not able to reproduce change from transition boiling regime to nucleate boiling regime, which is

by the air/water spray from initial temperature of 600 °C. Time dependent temperature change was measured on the opposite side with the aim of infrared thermography. Distance of the nozzle from the specimen varied, whereas this work deals with case where it was 200 mm. More details can be found in [6].

The same hexahedron mesh from previous section was used. On the outlet of

Along with the default case, sensitivity analysis was performed in which following parameters were varied: number of spray wall interaction regimes, droplet size, droplet velocity and wall heat penetration coefficient. In the following figures it can be seen that all simulation results are underestimating heat transfer process during spray quenching. Default case represents droplet

clearly observable in experiment as steep slope of the cooling curve around 0.8 second. It can be concluded that new models are necessary in order to accurately represent effects of spray quenching, such as correlation of Wendelstorf *et al.* [29].

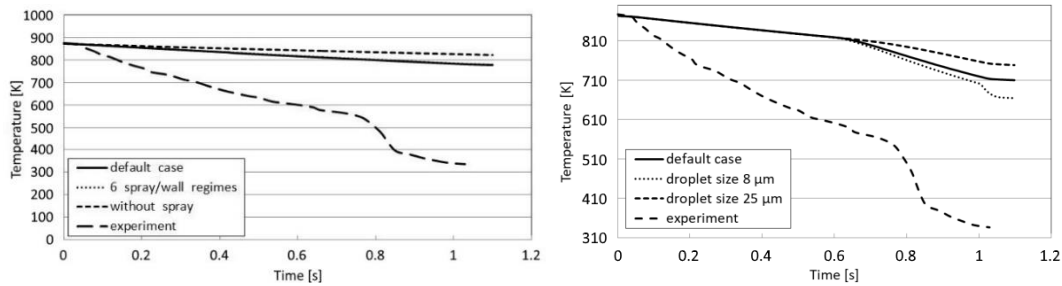


Figure 3. Influence of impingement regimes (left) and droplet size (right) on the heat transfer during spray quenching process

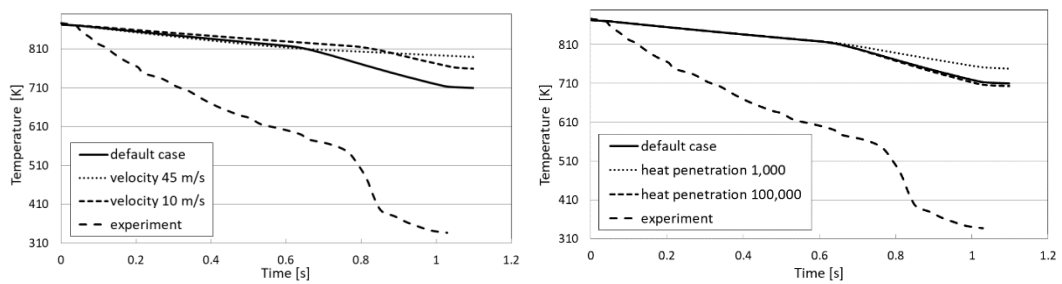


Figure 4. Influence of droplet velocity (left) and wall heat penetration coefficient (right) on the heat transfer during spray quenching process

Simulation with new heat transfer coefficient correlation

Although correlation of Wendelstorf *et al.* [29] has been already implemented in the work of Edelbauer *et al.* [28], this has been realized in the framework of Eulerian multiphase approach. Present work includes adjustment of correlation for the purposes of Lagrangian spray approach which is still prevailing in industrial applications. For the simulation the same numerical settings as reported in previous section were retained.

Figure 5 presents first results of implemented heat transfer correlation compared with quenching curve reproduced from correlation itself, rationale for which has been given in section *Quenching heat transfer coefficient*. It can be seen that surface temperature is following trend obtained by experiment and verifies implemented model. Compared to the

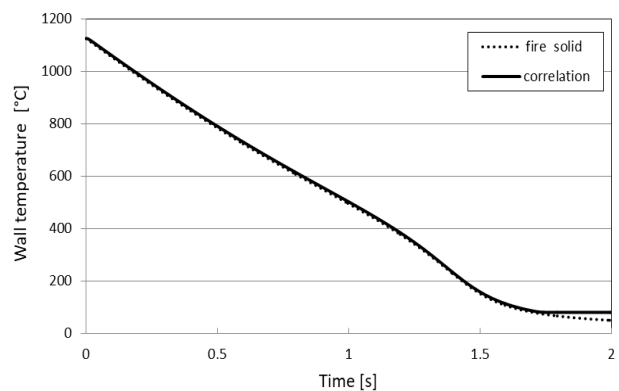


Figure 5. First results of correlation from Wendelstorf *et al.* [29] implemented in CFD code

available model it can be clearly seen that now it is possible to simulate dense spray quenching applications. It should be noticed that correlation also captures change from transition boiling regime to nucleate boiling regime, which is manifested as a change of quenching curve slope after approx. 1.2 second.

Conclusions

The object of this research was numerical investigation of spray quenching process with the aim of determination whether existing models implemented in commercial CFD code Fire are able to represent heat transfer dynamics. After mathematical framework was presented, simulation settings were given together with discussion of results. Sensitivity analysis was performed where number of spray wall interaction regimes, droplet size, droplet velocity and wall heat penetration coefficient were varied. All simulation results underestimated heat transfer process during spray quenching, which brought the conclusion that existing droplet/wall heat transfer model is maybe able to reproduce heat transfer of dilute spray but is unable to cope with effects of pronounced wall wetting. In order to overcome this difficulty, more accurate heat transfer model in Lagrangian spray approach on the basis of correlation by Wendelstorf *et al.* [29] was developed. Correlation was used to calculate heat source for liquid phase which is at the same time heat sink for hot wall. First results of heat transfer from solid indicate favorable outcome, whereas simulation was also successful to capture change from transition boiling regime to nucleate boiling regime.

Recommendations for future work consist of implementation of correlations for twin fluid atomizers that are gaining in popularity in recent times, as well as implementation of most accurate correlations piecewise for each distinct heat transfer regime.

Nomenclature

A – surface area, [m²]
 b – heat penetration coefficient, [Ws^{0.5}m⁻²K⁻¹]
 C – model constant, [-]
 D – diameter, [m]
 F – force, [N]
 f – mass force, [ms⁻²]
 i – specific internal energy of fluid, [Jkg⁻¹]
 K – non-dimensional velocity, [-]
 m – mass, [kg]
 p – pressure, [Pa]
 Q – heat, [J]
 S – source term, [-]
 T – temperature, [K]
 T^* – non-dimensional temperature, ($= T_w/T_s$), [-]
 t – time, [s]
 u – velocity, [ms⁻¹]
 V – volume, [m³]
 x_i – Cartesian space co-ordinates, [m]

Greek symbols

α – heat transfer coefficient, [Wm⁻²K⁻¹]

Γ – diffusion coefficient of scalar transport variable, [-]
 λ – thermal conductivity, [Wm⁻¹K⁻¹]
 μ – dynamic viscosity, [Pas]
 ρ – density, [kgm⁻³]
 σ – surface tension, [Nm⁻¹]
 τ_{ij} – viscous stress tensor, [Nm⁻²]
 φ – scalar transport variable, [-]

Subscripts

φ – related to scalar transport variable
 b – other external contributions
 cont – contact
 d – droplet
 dr – drag
 g – gravity and buoyancy
 p – pressure
 S – surface, saturation
 W – wall
 \perp – normal component

References

- [1] Anandan, S., Ramalingam, V., Thermal Management of Electronics: A Review of Literature, *Thermal Science*, 12 (2008), 2, pp. 5-26

- [2] Zdravec, M., et al., Cooling Analysis of a Light Emitting Diode Automotive Fog Lamp, *Thermal Science*, 21, (2017), 1, pp. 757-766
- [3] Smakulski, P., Pietrowicz, S., A Review of the Capabilities of High Heat Flux Removal by Porous Materials, Microchannels and Spray Cooling Techniques, *Appl. Therm. Eng.*, 104 (2016), July, pp. 636-646
- [4] Liang, G., Mudawar, I., Review of Spray Cooling – Part 2: High Temperature Boiling Regimes and Quenching Applications, *Int. J. Heat Mass Transf.*, 115 (2017), Part A, pp. 1206-1222
- [5] Yao, S. C., Cox, T. L., A General Heat Transfer Correlation for Impacting Water Sprays on High-Temperature Surfaces, *Exp. Heat Transf.*, 15 (2002), 4, pp. 207-219
- [6] Puschmann, F., Specht, E., Transient Measurement of Heat Transfer in Metal Quenching with Atomized Sprays, *Exp. Therm. Fluid Sci.*, 28 (2004), 6, pp. 607-615
- [7] Jha, J. M., et al., Heat Transfer from a Hot Moving Steel Plate by Air-Atomized Spray Impingement, *Exp. Heat Transf.*, 29 (2016), 1, pp. 78-96
- [8] Chen, R.-H., et al., Optimal Spray Characteristics in Water Spray Cooling, *Int. J. Heat Mass Transf.*, 47 (2004), 23, pp. 5095-5099
- [9] Chen, R.-H., et al., Effects of Spray Characteristics on Critical Heat Flux in Subcooled Water Spray Cooling, *Int. J. Heat Mass Transf.*, 45 (2002), 19, pp. 4033-4043
- [10] Silk, E. A., et al., Spray Cooling of Enhanced Surfaces: Impact of Structured Surface Geometry and Spray Axis Inclination, *Int. J. Heat Mass Transf.*, 49 (2006), 25-26, pp. 4910-4920
- [11] Ciofalo, M., et al., Investigation of the Cooling of Hot Walls by Liquid Water Sprays, *Int. J. Heat Mass Transf.*, 42 (1999), 7, pp. 1157-1175
- [12] Visaria, M., Mudawar, I., Effects of High Subcooling on Two-phase Spray Cooling and Critical Heat Flux, *Int. J. Heat Mass Transf.*, 51 (2008), 21-22, pp. 5269-5278
- [13] Mascarenhas, N., Mudawar, I., Analytical and Computational Methodology for Modeling Spray Quenching of Solid Alloy Cylinders, *Int. J. Heat Mass Transf.*, 53 (2010), 25-26, pp. 5871-5883
- [14] Al-Ahmadi, H. M., Yao, S. C., Spray Cooling of High Temperature Metals Using High Mass Flux Industrial Nozzles, *Exp. Heat Transf.*, 21 (2008), 1, pp. 38-54
- [15] Liang, G., Mudawar, I., Review of Spray Cooling – Part 1: Single-Phase and Nucleate Boiling Regimes, and Critical Heat Flux, *Int. J. Heat Mass Transf.*, 115 (2017), Part A, pp. 1174-1205
- [16] Zhao, R., et al., Study on Heat Transfer Performance of Spray Cooling: Model and Analysis, *Heat Mass Transf.*, 46 (2010), 8-9, pp. 821-829
- [17] Shedd, T. A., Pautsch, A. G., Spray Impingement Cooling with Single- and Multiple-nozzle Arrays, Part II: Visualization and Empirical Models, *Int. J. Heat Mass Transf.*, 48 (2005), 15, pp. 3176-3184
- [18] Mascarenhas, N., Mudawar, I., Methodology for Predicting Spray Quenching of Thick-Walled Metal Alloy Tubes, *Int. J. Heat Mass Transf.*, 55 (2012), 11-12, pp. 2953-2964
- [19] Mudawar, I., Estes, K. A., Optimizing and Predicting CHF in Spray Cooling of a Square Surface, *J. Heat Transfer*, 118 (1996), 3, pp. 672-679
- [20] Visaria, M., Mudawar, I., Theoretical and Experimental Study of the Effects of Spray Inclination on Two-phase Spray Cooling and Critical Heat Flux, *Int. J. Heat Mass Transf.*, 51 (2008), 9-10, pp. 2398-2410
- [21] Tseng, A. A., et al., Liquid Sprays for Heat Transfer Enhancements: A Review, *Heat Transf. Eng.*, 37 (2016), 16, pp. 1401-1417
- [22] Benmouhoub, D., Mataoui, A., Computation of Heat Transfer of a Plane Turbulent Jet Impinging a Moving Plate, *Thermal Science*, 18 (2014), 4, pp. 1259-1271
- [23] Wang, J., et al., Effect of an Upstream Bulge Configuration on Film Cooling with and without Mist Injection, *J. Environ. Manage.*, 203 (2017), Part 3, pp. 1072-1079
- [24] Ban, M., Duic, N., Adaptation of n-heptane Autoignition Tabulation for Complex Chemistry Mechanisms, *Thermal Science*, 15 (2011), 1, pp. 135-144
- [25] Qi, F., et al., Numerical Study and Structural Optimization of a Top Combustion Hot Blast Stove, *Adv. Mech. Eng.*, 7 (2015), ID 709675
- [26] Petranović, Z., et al., Modelling Pollutant Emissions in Diesel Engines, Influence of Biofuel on Pollutant Formation, *J. Environ. Manage.*, 203 (2017), Part 3, pp. 1038-1046
- [27] Mikulčić, H., et al., Numerical Analysis of Cement Calciner Fuel Efficiency and Pollutant Emissions, *Clean Technol. Environ. Policy*, 15 (2013), 3, pp. 489-499
- [28] Edelbauer, W., et al., Numerical and Experimental Investigation of the Spray Quenching Process with an Euler-Eulerian Multi-Fluid Model, *Appl. Therm. Eng.*, 100 (2016), May, pp. 1259-1273

- [29] Wendelstorf, J., *et al.*, Spray Water Cooling Heat Transfer at High Temperatures and Liquid Mass Fluxes, *Int. J. Heat Mass Transf.*, *51* (2008), 19-20, pp. 4902-4910
- [30] Yuen, M. C., Chen, L. W., On Drag of Evaporating Liquid Droplets, *Combust. Sci. Technol.*, *14* (1976), 4-6, pp. 147-154
- [31] Mikulčić, H., *et al.*, Numerical Evaluation of Different Pulverized Coal and Solid Recovered Fuel Co-firing Modes Inside a Large-Scale Cement Calciner, *Appl. Energy*, *184* (2016), Dec., pp. 1292-1305
- [32] Petranović, Z., *et al.*, Modelling of Spray and Combustion Processes by Using the Eulerian Multiphase Approach and Detailed Chemical Kinetics, *Fuel*, *191* (2017), Mar., pp. 25-35
- [33] Kuhnke, D., *Spray Wall Interaction Modelling by Dimensionless Data Analysis*, Shaker Verlag GmbH, Herzogenrath, Germany, 2004
- [34] Wruck, N., *Transient Boiling by Drops on Wall Impact*, RWTH Aachen, Aachen, Germany, 1999
- [35] Abramzon, B., Sirignano, W. A., Droplet Vaporization Model for Spray Combustion Calculations, *Int. J. Heat Mass Transf.*, *32* (1989), 9, pp. 1605-1618